Effect of thermistor on wavelength variation of superluminescent diode over the whole operating temperature range

SHUAI ZHOU*, XUE-YANG ZHANG, CHEN FENG, JING ZHANG, ZU-RONG TANG, TAO REN, LIN KUANG, WEI LI

Chongqing Optoelectronics Research Institute, Chongqing 400060, People's Republic of China

A unilateral 6-pin butterfly packaging superluminescent diode module was fabricated, and the mean wavelength variation was measured under different ambient temperatures, i.e. 298.15K, 228.15K and 343.15K. Under 228.15K, the mean wavelength is longer than that under 298.15K, and under 343.15K, the mean wavelength is shorter than that under 298.15K. Simulation result shows that the resistance distribution of thermistor is easily affected by ambient temperature which is due to a low thermal conductivity, even though there is a thermoelectric cooler which controls the operating temperature of superluminescent diode chip. To ensure that the thermistor resistance value is 10KΩ, the thermoelectric cooler has to heat at 228.15K and cool at 343.15K. A method of reducing the thickness of thermistor to decreasing the maximum temperature difference in whole operating temperature range is proposed, which is necessary for decreasing the wavelength variation of superluminescent diode module.

(Received July 24, 2024; accepted December 2, 2024)

Keywords: Superluminescent diode, Thermistor, Wavelength variation, Thermal conductivity

1. Introduction

Due to broad emission spectra and high power, superluminescent diode (SLD) has been widely used in optical coherence tomography (OCT)[1], optical low-coherence reflectometry (OLCR)[2], truly random number generation (TRNG)[3], and especially fiber-optic gyroscope (FOG) [4, 5]. FOG is based on optical fiber Sagnac principle [6]. For example, a typical closed-loop FOG system has two main components, optical path and circuit module [7]. The optical path part includes the broad-band light source, coupler, Y-waveguide, fiber coil and photodetector [8], as shown in Fig. 1. The circuit module includes amplifier, A/D converter, D/A converter, digital demodulation circuit, digital controller circuit and digital filtering. Different from many other optical systems which require narrow-band light sources, FOG requires broad-band, high-power sources to reduce coherent errors. The requirements of light sources for FOG are [9-12]: (1) The spectrum band of source must be broad in order to minimize errors due to coherence effects; (2) The source must produce adequate power in a single spatial mode, which can be efficiently coupled into a single-mode fiber. High power will improve the signal to noise ratio (SNR) of FOG; (3) The mean wavelength of the light source must be stable, which will influence the FOG scale factor (SF); (4) Reliability.

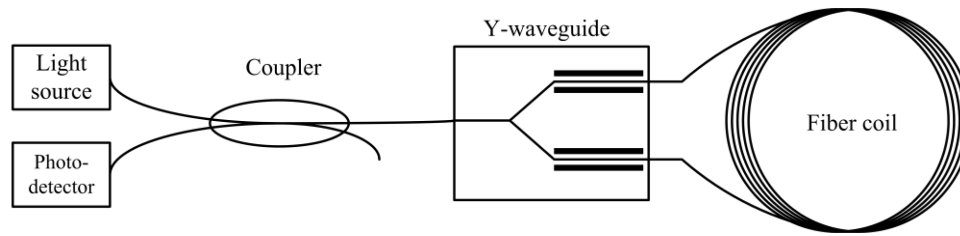

Fig. 1. Sketches of the optical path part of FOG

Three kinds of broadband light sources have been used in FOG technology, i.e., light-emitting diode (LED), SLD and erbium-doped superfluorescent fiber source (SFS). The power of LED is usually lower, and LED is needed to reduce the noise component of the output signal of an FOG [13]. SLD is required in FOG due to both their broad emission spectrum and high power [14]. Although, the stability of mean wavelength of SFS is better than SLD source, which leads to smaller SF error [7]. The main advantage of SLD is processability, and hence relatively low cost. However, SF is one of the important parameters in FOG test, and SF error affects the accuracy of the FOG. The SF can be expressed as follows [7],

$$SF = \frac{2\pi LD}{\lambda K_{DA} K_4 c} \tag{1}$$

where L is the length of fiber, D is the diameter of fiber coil, λ is the mean wavelength of broadband light source, K_{DA} is the coefficient of D/A converter, K_4 is the modulation coefficient of post-amplifier. The change in mean wavelength of SLD is one of the influencing factors of SF error.

The main parameters that affect the mean wavelength of SLD are current and temperature. Normally, during the operation of FOG, SLD works in constant current mode, ensuring that the mean wavelength is not easily affected by current changes. In addition, the mean wavelength of SLD chip is a temperature-sensitive parameter, hence thermoelectric cooler (TEC) and thermistor are needed to ensure that the SLD chip operates at a constant temperature in a butterfly package. Some papers have reported the effects of thermistor on performance of butterfly package lasers. Yin *et al*. proposed that the farther distance between thermistor and SLD chip will bring an obvious time delay to the SLD transfer function and a closer relationship between SLD and differential parameter [15]. Gao *et al.* demonstrated that, in the packaging process of optoelectronic devices for high speed applications, reducing the height of thermistor can increase the temperature detecting speed, which is necessary when the response of the sub-mount is fast [16]. Eason *et al.* proposed that the thermistor location will influence the measured temperature and thermal response time of the photonic package, but it can still follows the device temperature well enough to provide the thermoelectric module controller with adequate feedback to maintain the device at a steady temperature in steady state running condition [17]. However, the effect of thermistor on mean wavelength variation of superluminescent diode over the whole operating temperature range is rarely reported.

In this work, we studied the variation characteristics of the mean wavelength of SLD modules with temperature. In section 2, theoretical aspect and fabrication process are described. In section 3, experimental and simulation results are described and discussed. In section 4, the results of this paper are summarized and conclusions are given. The objective of this work was to provide a reference to optimize wavelength stability of SLD modules.

2. Fundamental theory and experimental section

Chips used in this work were InGaAsP/InP bulk-material buried-heterojunction (BH) SLDs as mentioned in Ref. [18]. The wavelength of SLD is closely related to the band-gap energy of active region materials. The relationship between wavelength and band-gap energy could be expressed as $\lambda \approx 1.24/E_g$[19]. The simplest relation of band-gap energy for InxGa1-xAsyP1-y at room temperature is derived from four binary band-gap

parameters as follow [20]:

$$E_g(x,y) = x(1-y)E_{g,InP} + xyE_{g,InAs} + (1-x)(1-y)E_{g,GaP} + (1-x)yE_{g,GaAs} \quad (2)$$

$E_{g,X}$ is the binary band-gap energy, and considering the equation of temperature dependence of band-gap by Varshni formula [21],

$$E_g(T) = E_g(0) - \frac{\alpha T^2}{T+\beta} \quad (3)$$

where $E_g(0)$ is the band-gap energy at zero Kelvin, α and β are the coefficients. The parameters of corresponding four binary alloys are listed in Table 1.

Table 1. Overview of the parameters of binary alloys

Binary Alloy	$E_g(0)$ (eV)	α (eV/K)	β (K)
InP[20]	1.421	3.63×10^{-4}	162
InAs[20]	0.420	2.5×10^{-4}	75
GaP[22]	2.338	6.2×10^{-4}	460
GaAs[20]	1.519	5.405×10^{-4}	204

Both the SLD chip and thermistor are soldered to AlN submount, and the distance between the two is about 200 microns. The thermistor is composed of a piece of thermo-sensitive material sandwiched by two metal electrodes. The lower electrode is mounted on AlN heat-sink by the $Au_{80}Sn_{20}$ eutectic welding process, and the gold bonding wire is used to connect the upper electrode of thermistor to the Pin of butterfly package. The dimension of thermistor is $0.32\times0.32\times0.25mm^3$. The thermistor coefficients A, B, and C linearize the thermistor temperature-resistance curve and are related using the Steinhart and Hart equation as follows:

$$\frac{1}{T} = A + B(\ln R) + C(\ln R)^3 \quad (4)$$

where T is the temperature (K), R is the Thermistor resistance (Ω). A, B and C are the thermistor coefficients, and the values of thermistor coefficients used in this work are 1.1115×10^{-3}, 2.345×10^{-4} and 8.21×10^{-8}, respectively.

A unilateral 6-pin butterfly packaging module was fabricated, which consists of SLD chip, thermistor, AlN submount, metallic plate, TEC and fiber subassembly, as is shown in Fig. 2. The SLD chip was mounted on the cold-side of TEC along with thermistor, submount and metallic plate. The hot-side of TEC was soldered in the butterfly housing. Then the SLD chip was controlled to operate at about 298.15K. The fiber ferrule, saddle-shaped clip, and metallic plate were joined by YAG laser welding, ensuring that the output light from SLD chip could be stably coupled into the fiber. The thermistor and TEC were controlled by an autotuning TEC sourcemeter instrument, and a stabilized direct current (DC) was injected into the SLD chip by a sourcemeter instrument. The SLD module was put into a high-low temperature test chamber, and the mean wavelength was measured by YOKOGAWA AQ6370 optical spectrum analyzer.

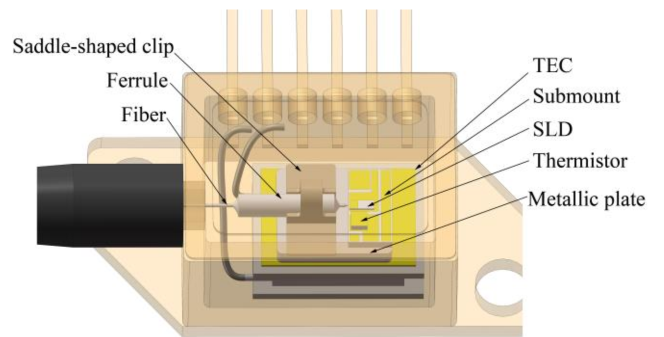

Fig. 2. Schematic structure of the unilateral 6-pin butterfly packaging module (color online)

3. Result and discussion

The measured relationship of mean wavelength with temperature changes around 298.15K is shown in Fig. 3. The mean wavelengths of two SLD butterfly packaged

modules were measured from 294.15K to 303.15K, and 100mA DC was injected into the SLD chips. During testing, the TEC in module was used to control temperature changes to alter the working environment temperature of SLD chips. Then the slopes of mean wavelength variation with temperature are 0.433nm/K (red circles) and 0.459nm/K (blue squares), respectively. The calculated slope of wavelength vs. temperature (black triangles) is about 0.447nm/K, which is almost consistent with the experimental results. The temperature-dependent dilatation of lattice and electron lattice interaction is the mechanism that how temperature affects the band-gap energy [23]. Finally, the change in band-gap leads to the change in wavelength.

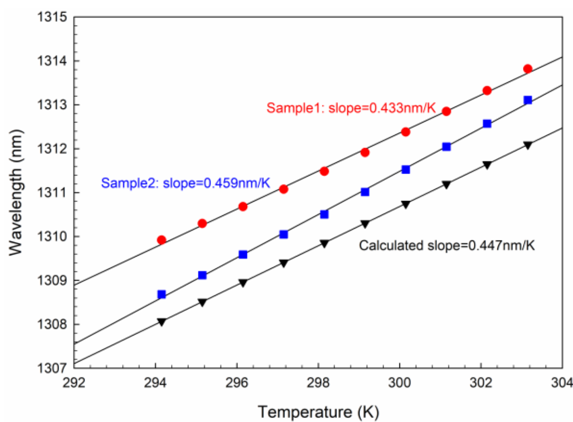

Fig. 3. Wavelength-temperature curves for two measured samples and calculated result (color online)

In order to study the wavelength variation characteristics over the whole operating temperature range, there SLD modules (sample 1, sample 2 and sample 3) were put into a temperature cycling test chamber. 100mA DC was injected into the SLD chip and the resistance value of thermistor was controlled at 10KΩ (i.e. 298.15K) by autotuning TEC sourcemeter instrument. The temperature of test chamber changed from 298.15K to 228.15K and then to 343.15K. As is shown in Fig. 4, the mean wavelengths of sample1 at 298.15K, 228.15K and 343.15K are 1310.692nm, 1310.481nm and 1310.329nm, respectively. When the ambient temperature decreases, the mean wavelength shifts towards longer wavelength, and when the ambient temperature increases, the mean wavelength shifts towards shorter wavelength, as shown in the inset of Fig. 4. Based on the characteristics of wavelength changes, as shown in Fig. 3, in high-temperature environment, the temperature of SLD chip is controlled below 298.15K, and in low-temperature environment, the temperature of SLD chip is controlled above 298.15K. However, the controlled temperature values of autotuning TEC sourcemeter instrument were all 298.15K at three test chamber temperatures.

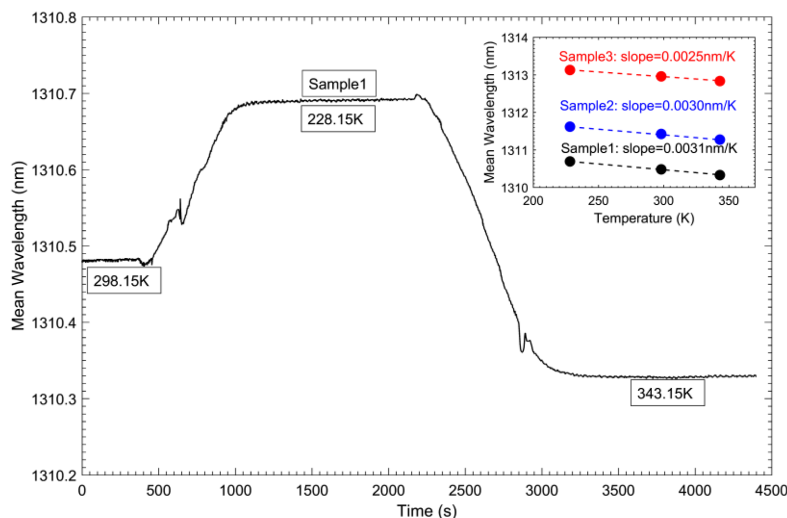

Fig. 4. Mean wavelength of SLD modules (sample 1, 2 and 3) under different ambient temperatures (color online)

To explain the cause of the phenomenon in Fig. 4, we used finite element analysis (FEA) to simulate the

temperature distribution of the chip on carrier (COC, i.e. SLD chip, thermistor, submount and metallic plate) in high and low temperature environments, respectively. To simplify the simulation, a constant temperature of 298.15K was added to the bottom of metallic plate, and the SLD chip was in a non-working state. The thermal convection was $5Wm^{-2}K^{-1}$. As shown in Fig. 5(a) and 5(b), the minimum and maximum temperature of the COC are 298.1K and 298.4K when the ambient temperature is set to 343.15K. As shown in Fig. 5(c) and 5(d), the minimum and maximum temperature of the COC are 297.7K and 298.1K when the ambient temperature is 228.15K. The temperature change mainly occurs on the thermistor, and the total temperature difference is about 0.7K. This is because the thermistor has the minimum thermal conductivity. The thermal conductivity for the Metallic plate, AlN submount, InP chip, thermistor are $43Wm^{-1}K^{-1}$, $320Wm^{-1}K^{-1}$, $80Wm^{-1}K^{-1}$, and $0.6Wm^{-1}K^{-1}$[16], respectively. Although there is a temperature controller, the temperature of thermistor is more easily affected by the ambient temperature comparing to other components. Fig. 6 shows the maximum temperature difference △T of thermistor with assumed thermal conductivity.

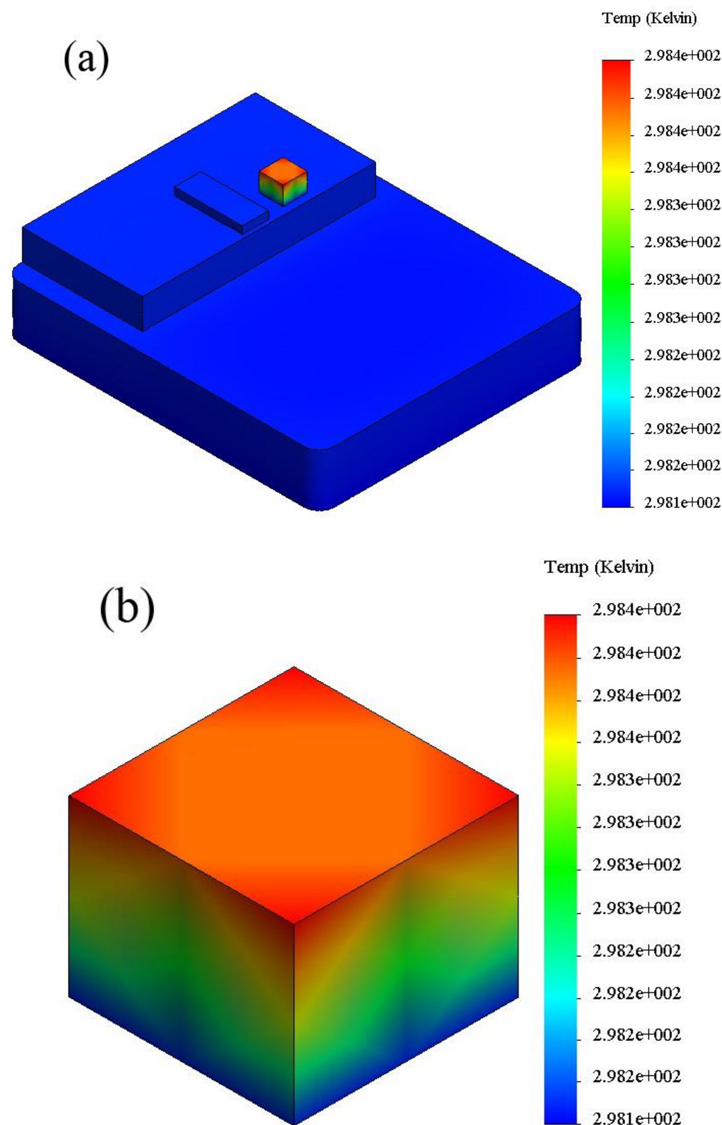

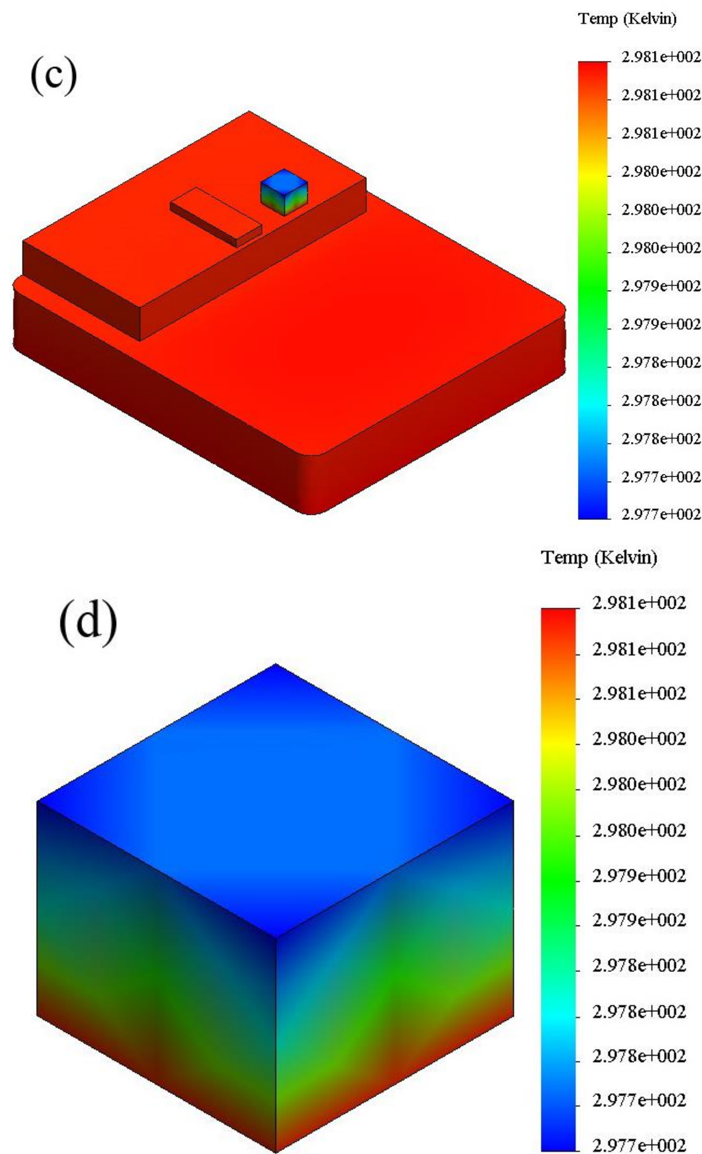

Fig. 5. The temperature distributions of COC with 0.32 ×0.32 ×0.25mm^3 thermistor under 343.15K (a) and 228.15K (c), and the partial diagram of thermistor under 343.15K (b) and 228.15K (d) (color online)

The results prove that, under high-temperature environment, the temperature on top-side of the thermistor is higher than that on the bottom-side, and under low-temperature environment, the temperature on top-side of the thermistor is lower than that on the bottom-side. The thermo-sensitive material used is negative temperature coefficient (NTC) material and the resistance of thermistor at 298.15K is 10KΩ. Assuming the thermistor is composed of several resistors connected in series. Under 298.15K, the distribution of resistance is uniform and the total resistance is 10KΩ. Under 228.15K, the distribution of resistance is non-uniform and the resistance on top-side of the thermistor is higher than that on the bottom-side. To ensure that the total resistance of thermistor is 10KΩ, TEC must heat, so that the resistance on bottom-side of thermistor decreases and the wavelength of SLD chip shifts towards longer wavelength. Under 343.15K, the resistance on top-side of the thermistor is lower than that on the bottom-side. To ensure that the total resistance of thermistor is 10KΩ, TEC must cool, so that the resistance on bottom-side of thermistor increases and the wavelength of SLD chip shifts towards shorter wavelength.

To reduce the wavelength variation of superluminescent diode module over the whole operating

temperature range, this work proposes that a thinner thermistor will decrease the maximum temperature difference △T. This is because the temperature on top-side of a thick thermistor is more easily affected by the ambient temperature than that of a thin thermistor. The simulation results of temperature distributions for COC with a $0.45\times0.45\times0.18mm^3$ thermistor under 343.15K and 228.15K are shown in Fig. 7. The maximum temperature difference △T of thermistor is about 0.4K, which is 0.3K less than that of $0.32\times0.32\times0.25mm^3$ thermistor. To verify the simulation results, another three samples were fabricated with the thinner thermistor, i.e. sample 4, sample 5 and sample 6. The change rates of mean wavelength with ambient temperature for sample 1 and sample 4 are shown in Fig. 8. The total change rates for sample 1 and sample 4 from 228.15K to 343.15K are about 277.7ppm and 129.5ppm. The measured results show a significantly decrease in wavelength variation of superluminescent diode module over the whole operating temperature range. As shown in the insets of Fig. 4 and Fig. 8, the average slopes are 0.00287nm/K and 0.00137nm/K, respectively.

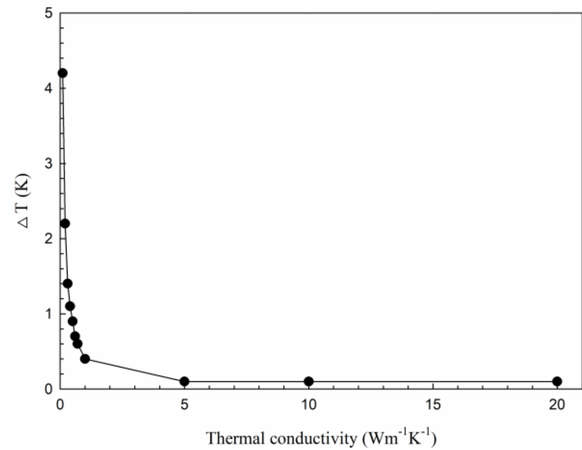

Fig. 6. The maximum temperature difference of thermistor with its thermal conductivity

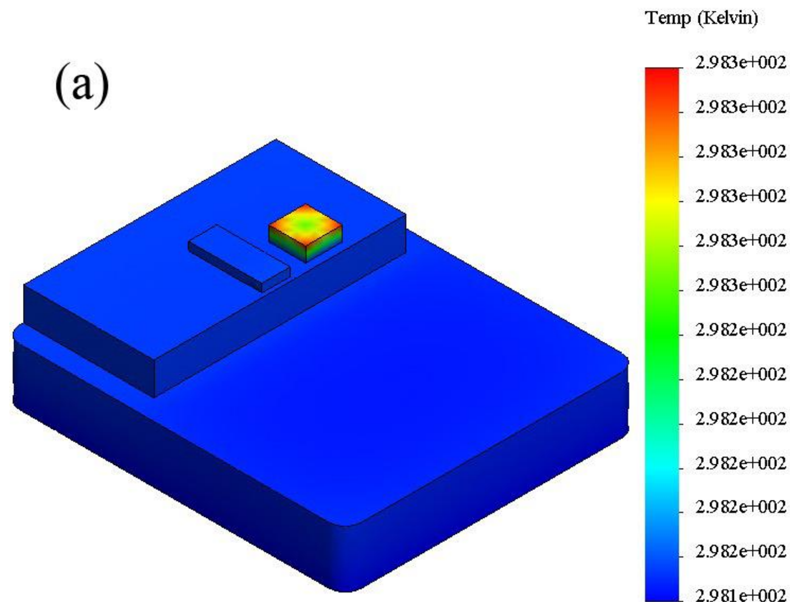

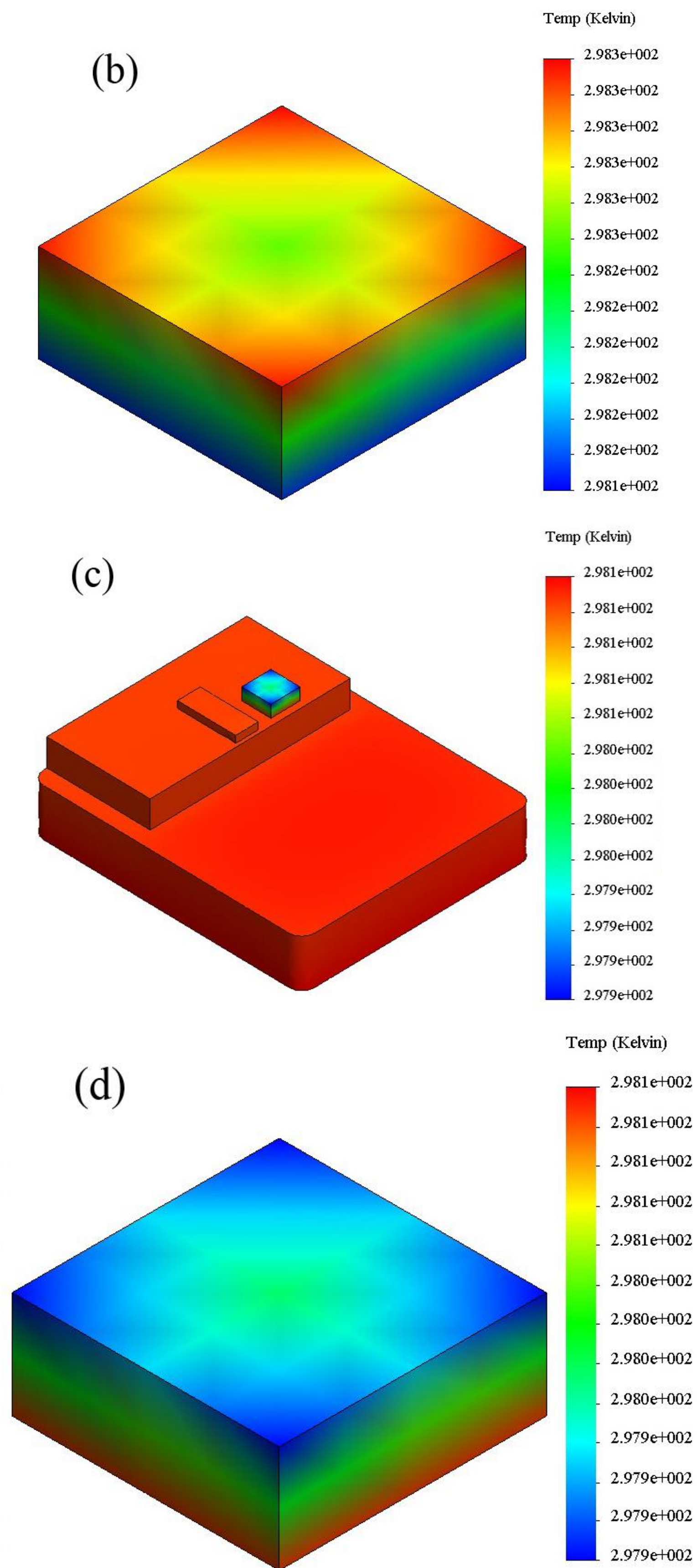

Fig. 7. The temperature distributions of COC with 0.45×0.45×0.18mm³ thermistor under 343.15K (a) and 228.15K (c), and the partial diagram of thermistor under 343.15K (b) and 228.15K (d) (color online)

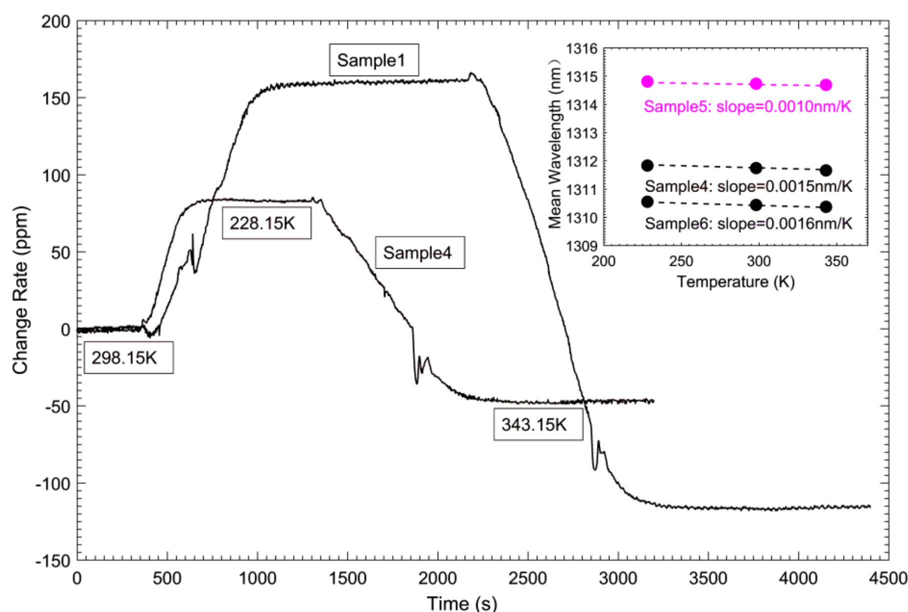

Fig. 8. Mean wavelength of SLD modules (sample 4, 5 and 6) under different ambient temperatures (color online)

4. Conclusion

In this work we devoted to studying the variation characteristics of the mean wavelength of SLD modules from 228.15K to 343.15K, and unilateral 6-pin butterfly packaging modules were fabricated. We have analyzed the principle of wavelength variation of SLD chip with temperature and the average value of measured slopes of mean wavelength variation with temperature is about 0.446nm/K. Then, the SLD modules were put into a temperature cycling test chamber and the wavelength variation characteristics with ambient temperature were measured. The high ambient temperature results in blue-shift in mean wavelength and the low ambient temperature results in red-shift in mean wavelength. The reason of this phenomenon is the change of thermistor resistance distribution with ambient temperature. A method of reducing the thickness of thermistor to decreasing the maximum temperature difference in whole operating temperature range is proposed, which is necessary for decreasing the wavelength variation of SLD module. These results could be useful for SLD module design.

Acknowledgements

This work was supported by Chongqing Optoelectronics Research Institute.

References

[1] C. Thanomsit, J. Saetiew, P. Meemon, Toxicol. Rep. **9**, 181 (2022).

[2] S. Cattini, L. Rovati, J. Lightwave Technol. **39**(12), 3771 (2020).

[3] Y. Liu, M. Zhu, B. Luo, J. Zhang, H. Guo, Laser Phys. Lett. **10**, 045001 (2013).

[4] J. Zhang, X. Liu, Y. Niu, L. Ma, K. Wang, M. Ding, Opt. Express **28**(7), 9359 (2020).

[5] Z. Tian, C. Lei, G. Liu, S. Zhou, Y. Hua, Semiconductor Optoelectronics **40**(3), 343 (2019).

[6] X. Dong, H. Tam, P. Shum, Appl. Phys. Lett. **90**, 151113 (2007).

[7] X. Li, M. Li, C. Liu, H. Li, H. Yang, Optik **242**, 167189 (2021).

[8] J. Mou, T. Huang, X. Shu, Opt. Fiber Technol. **60**, 102368 (2020).

[9] P. Wysocki, M. Digonnet, B. Kim, H. Shaw, J. Lightwave Technol. **12**(3), 550 (1994).

[10] M. Li, X. Huang, J. Jin, Y. Chen, R. Kang, Trans.

Jpn. Soc. Aeronaut. Space Sci. **55**(2), 89 (2012).

[11] P. Ou, B. Cao, C. Zhang, Y. Li, Y. Yang, Electron. Lett. **44**(3), 187 (2008).

[12] S. Zhou, J. Xu, K. Tian, J. Zhang, F. Pang, S. Liu, T. Ren, K. Liao, Semiconductor Optoelectronics **42**(4), 483 (2021).

[13] G. Sandoval-Romero, J. Opt. Technol. **74**(8), 573 (2007).

[14] S. Zhou, Z. Tang, S. Liu, Y. Zhou, J, Zhang, L. Duan, K. Tian, K. Zhao, C. Feng, Phys. Status Solidi A **215**, 1800176 (2018).

[15] J. Yin, C. Xu, B. Zhou, Y. Chen, Optical Technique **41**(3), 217 (2015).

[16] J. Gao, X. Han, Y. Yu, 2015 16th International Conference on Electronic Packaging Technology (ICEPT), 8 (2016).

[17] C. Eason, M. Rensing, J. S. Lee, P. O'Brien, J. Phys.: Conf. Ser. **525**, 1 (2014).

[18] S. Zhou. Int. J. Mod. Phys. B **31**, 1750229 (2017).

[19] S. Chuang, Physics of Optoelectronic Devices, Wiley (1995).

[20] E. Li, Phys. E **5**, 215 (2000).

[21] Y. Varshni, Physica **34**(1), 149 (1967).

[22] M. Panish, J. Casey, J. Appl. Phys. **40**(1), 163 (1969).

[23] K. O'Donnell, X. Chen, Appl. Phys. Lett. **58**(25), 2924 (1991).

*Corresponding author: zscetc44@gmail.com